Multistate Reactivity in Styrene Epoxidation by Compound I of Cytochrome P450: Mechanisms of Products and Side Products Formation

Devesh Kumar,[a] Sam P. de Visser,*[b] and Sason Shaik*[a]

Abstract: Density functional theoretical calculations are used to elucidate the epoxidation mechanism of styrene with a cytochrome P450 model Compound I, and the formation of side products. The reaction features multistate reactivity (MSR) with different spin states (doublet and quartet) and different electromeric situations having carbon radicals and cations, as well as iron(III) and iron(IV) oxidation states. The mechanisms involve state-specific product formation, as follows: a) The low-spin pathways lead to epoxide formation in effectively concerted mechanisms. b) The high-spin pathways have finite barriers for ring-closure and may have a sufficiently long lifetime to undergo rearrangement and lead to side products. c) The high-spin radical intermediate, $^4\mathbf{2}_{rad}$-IV, has a ring closure barrier as small as the C−C rotation barrier. This intermediate will therefore lose stereochemistry and lead to a mixture of *cis* and *trans* epoxides. The barriers for the production of aldehyde and suicidal complexes are too high for this intermediate. d) The high-spin radical intermediate, $^4\mathbf{2}_{rad}$-III, has a substantial ring closure barrier and may survive long enough time to lead to suicidal, phenacetaldehyde and 2-hydroxostyrene side products. e) The phenacetaldehyde and 2-hydroxostyrene products both originate from crossover from the $^4\mathbf{2}_{rad}$-III radical intermediate to the cationic state, $^4\mathbf{2}_{cat,z^2}$. The process involves an *N*-protonated porphyrin intermediate that re-shuttles the proton back to the substrate to form either phenacetaldehyde or 2-hydroxostyrene products. This resembles the internally mediated NIH-shift observed during benzene hydroxylation.

Introduction

Cytochrome P450 enzymes (P450s) are heme enzymes that perform biotransformations, such as sterol synthesis, drug metabolism, and detoxification of xenobiotics.[1–7] The catalytic center of these enzymes is an iron protoporphyrin complex that is bound to the protein via a sulfur bridge of a cysteinate residue. The enzyme uses dioxygen to generate the active species, which is a high-valent oxoiron porphyrin complex, called Compound I (Cpd I, see Scheme 1). Cpd I catalyzes a variety of reactions, such as C=C double bond epoxidation, aliphatic C−H hydroxylation, desaturation, and heteroatom oxidation. This versatility of P450s has been one of the main reasons for the intense interest in the mechanistic understanding of their reactions.

One of the most widely used substrates to study the epoxidation reaction mechanism is styrene.[8–17] Styrene is epoxidized by synthetic oxo-metal porphyrin catalysts as well as by wild-type P450s.[18,19] In particular, Vaz et al.[19] measured rate constants for styrene epoxidation in several P450 isozymes and mutants, and estimated free energy barriers of 24–25 kcal mol^{-1}. Quite a few groups investigated also the stereoselectivity of product formation by, for example, using *cis*- or *trans*-methylstyrene.[18,20–24]

The enzymatic conversion of styrene into an epoxide, however, is not a clean reaction since it involves undesired side products, as shown in Scheme 1, which depicts along-

[a] Dr. D. Kumar, Prof. S. Shaik
Department of Organic Chemistry and the Lise Meitner-Minerva Center for Computational Quantum Chemistry
The Hebrew University of Jerusalem, 91904 Jerusalem (Israel)
Fax (+972)2-658-5345
E-mail: sason@yfaat.ch.huji.ac.il

[b] Dr. S. P. de Visser
School of Chemical Engineering and Analytical Science
University of Manchester
PO Box 88, Sackville Street, Manchester M60 1QD (UK)
Fax: (+44)161-306-4911
E-mail: sam.devisser@manchester.ac.uk
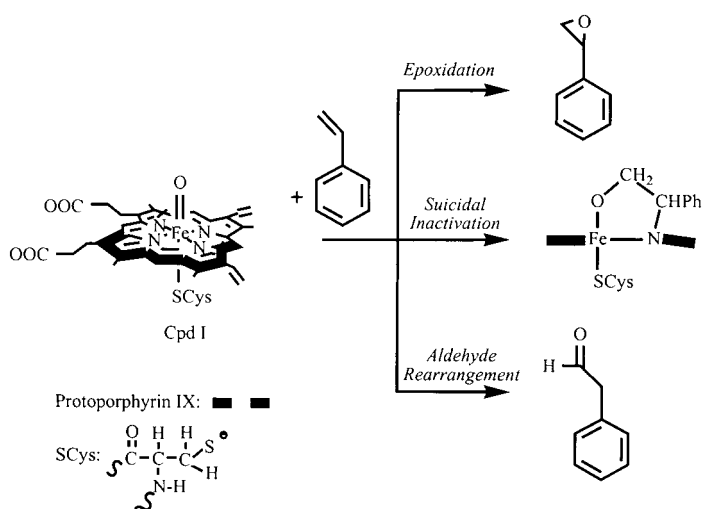
Scheme 1. Oxidation of styrene by Cpd I leading to epoxide and side products.

side the epoxide also phenacetaldehyde[10,17,18] and the *N*-alkylated porphyrin complex. The latter species, the so-called suicidal complex, destructs the catalyst/enzyme by forming dead-end products that do not allow regeneration of the active species. In particular, primary alkenes are known to produce these suicidal complexes.[1,3,5,6,25–32] Mechanistic studies have suggested that the reaction is stepwise or involves a stepwise branch with an intermediate[5,6,8,33] that generates the by-products. Two types of reaction intermediates, radicals and carbocations, are usually invoked to account for the side product formation, while the generally stereospecific epoxidation is thought to occur by a concerted oxygen transfer mechanism.

Studies of epoxidation of styrene and styrene derivatives using synthetic catalysts have revealed a wealth of information; some key conclusions follow. Chiral synthetic iron–porphyrin catalysts were made with different substituents on the *meso* position.[8] With styrene as a substrate, one of these catalysts produced the (*R*)-(+) isomer in 65% yield and in 31% enantiomeric excess, but also phenacetaldehyde was obtained in 16% yield. The large groups on the *meso* position caused steric hindrance for substrate binding and oxygen transfer and the degree of this steric hindrance determined the reactivity. The formation of aldehyde side products was studied, and control experiments ruled out that it originated from rearrangement of styrene-oxide. Accordingly, the formation of aldehyde must be competitive with epoxidation. Styrene derivatives with electron-withdrawing *para* substituents exhibited enhanced epoxidation/aldehyde ratios. This and other indications suggested the involvement of a cationic intermediate.

Collman et al.[10] studied the epoxidation of styrene and the formation of phenacetaldehyde side products with iron and manganese porphyrin systems. A product ratio of 4.6:1 of epoxide to phenacetaldehyde was obtained with (tetraphenylporphyrinato)manganese(III) chloride

(MnTPPCl) and a 14.3:1 product ratio was obtained with (tetrakis)(pentafluorophenyl)porphyrinatoiron(III) chloride (FePFPCl). Studies with isotopically labeled styrene proved that the hydrogen shift step that produces the aldehyde side product occurs after the rate-determining step since the yields of labeled and unlabeled epoxide versus aldehyde were the same. The experiments with [D_8]styrene showed retention of the labels, thus ruling out the assistance of solvent in the hydrogen shift step. Furthermore, the aldehyde production was found to be constant with time and therefore is a primary reaction product and does not arise from rearrangement of epoxide. It was thus concluded that both the epoxide and aldehyde products must originate from a common intermediate. This, however, has been disputed by other groups,[17] whose findings suggest that most of the phenacetaldehyde is formed not because of interference of the catalyst but is due to isomerization of the epoxide in the solvent. In addition, Collman et al.[10] investigated the epoxidation of *cis*-β-[D_1]styrene and *trans*-β-[D_1]styrene. The *cis*-β-[D_1]styrene–substrate produced both phenylacetaldehyde-1-[D] and phenylacetaldehyde-2-[D], indicating that both hydrogen and deuterium shifts took place. Although, the *cis*-β-[D_1]styrene gave dominant *cis*-epoxide and the *trans*-β-[D_1]styrene dominant *trans*-epoxide still both reactions exhibited some stereochemical scrambling (3–8% isomerization). It was suggested that the intermediate in the epoxidation reaction is presumably a radical species rather than a cationic one.

Experimental studies of Ortiz de Montellano et al. in combination of theoretical modeling of Loew et al. were carried out for styrene and methylstyrene epoxidation by P450$_{cam}$.[18,24] The docking studies[18] predicted similar product distribution as the experiments. Styrene activation by P450$_{cam}$ gave dominant styrene-oxide and phenacetaldehyde.[18] Another side product, benzaldehyde was thought to have originated from the reaction with uncomplexed H_2O_2. With 2-methylstyrene the authors reported, in addition to the epoxide, also *cis*-3-phenyl-2-propen-1-ol, a trace of 1-phenyl-2-propanone and minor amounts of aromatic ring hydroxylation side products.

Thus, the different studies point to a rich mechanistic scheme during C=C epoxidation,[6,7] with a variety of intermediates and unknowns, which depend on the substrate and the catalyst. In the case of styrene, for example, many studies suggest that all products are generated from a common intermediate. Some pieces of evidence point to a radical intermediate, while others point to a cationic intermediate, and still others suggest[17] that most of the phenacetaldehyde is formed due to isomerization of the epoxide in the solvent. Theory can be a helpful tool in defining more precisely mechanistic schemes. Previous density functional theory (DFT) studies on ethene[34–36] and propene[37] using a P450 model Cpd I species revealed a multistate scenario in which the different products are generated in a state-specific manner. All the low-spin state processes are effectively concerted epoxide-producing pathways. By contrast, all the high-spin processes are stepwise and lead either to an epox-

ide that does not conserve the isomeric identity of the alkene (*cis* and *trans* mixtures), or/and to by-products such as suicidal complexes and aldehydes. However, none of these theoretical studies dealt with a realistic substrate like styrene. Thus, the main goal of this paper is to use DFT to elucidate the mechanisms that lead to the formation of the three products in Scheme 1 during styrene epoxidation by Cpd I of P450.

Methods

All calculations presented here follow the same procedures as described in our previous work.[34,37–39] In brief, we use a DFT combination of the unrestricted hybrid density functional UB3LYP[40] with a double ζ basis set composed of LACVP[41a,b] on iron and the Pople-type 6–31G basis set[41c] on all the other atoms. The UB3LYP hybrid functional overestimates the stability of high-spin situations, but for the type of weakly coupled ferromagnetic and antiferromagnetic states as in Cpd I, it performs well.[42] The geometries of the species discussed later were fully optimized with the Jaguar program package[43] and subsequently verified by analytical frequency calculation using the Gaussian-98 program.[44] All local minima have real frequencies, while the transition states have one imaginary frequency. Free energies, whenever reported, were calculated from the frequency file in Gaussian for $T = 298.15$ K.

The active species (Cpd I) of Cytochrome P450 was mimicked as an oxoiron group embedded in a porphyrin ring without side chains and a thiolate axial ligand.[45] In addition, we tested the effect of two NH—S bonds to the thiolate ligand, using hydrogen-bonded ammonia molecules;[46,47] the orientation of these two ammonia molecules was taken from the optimized ^{4}CpdI·2NH$_3$ from reference [46] and here only single-point calculations were performed. Additionally, we ran single point calculations in a dielectric environment, having a dielectric constant of $\varepsilon = 5.7$, on the gas-phase geometries of the species, with and without two hydrogen bonded ammonia molecules. These calculations were done using the polarized continuum model (PCM) as implemented in Jaguar and used a probe radius of $r = 2.72$.[43] The complete project produced a great deal of data which are useful but not necessary to follow the thread of the paper; these data are supplied in the Supporting Information.

Results

Molecular orbitals along the reaction pathway: Before describing the results of the calculations let us begin with a brief presentation of the relevant orbitals in the reaction process. Figure 1 shows the high-lying occupied and low-lying virtual orbitals of Cpd I, **1**. The left-hand side of Figure 1 depicts the iron-type orbitals, which from bottom to top are the nonbonding δ orbital, the antibonding FeO orbitals π^*_{xz} and π^*_{yz}, and the antibonding orbitals with the other ligands σ^*_{xy} and $\sigma^*_{z^2}$. The δ orbital is doubly occupied in Cpd I and stays that way during the complete reaction. The two π* orbitals (π^*_{xz}, π^*_{yz}) are singly occupied in Cpd I. Together with the doubly occupied δ this corresponds to a d^4 electronic configuration, that is, a formal oxidation state Fe^{IV} on the iron. Another singly occupied orbital in Cpd I is the porphyrin type a$_{2u}$ orbital, which mixes strongly with the σ$_S$ orbital of the sulfur atom of the axial ligand. As such, Cpd I has a porphyrin cationic radical species, and can be described as Por$^+$·Fe^{IV}O.
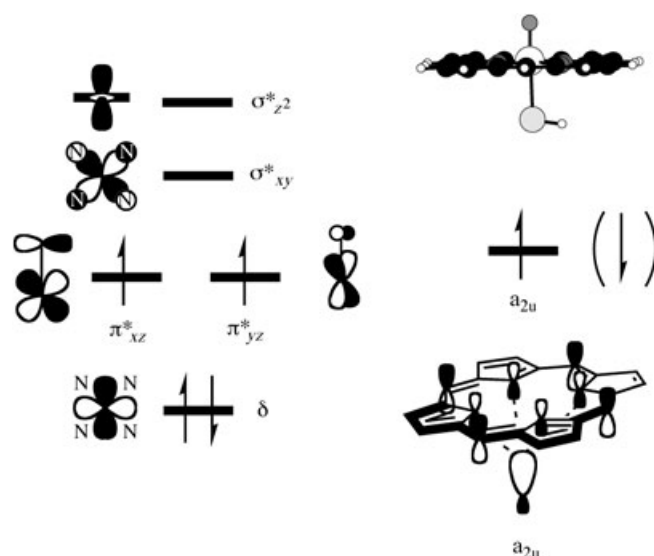

Figure 1. Some key orbitals of Cpd I, **1**, and occupancies in the quartet (doublet) states.

The oxidation of styrene by Cpd I involves a transformation from Por$^+$·Fe^{IV}O to PorFe^{III}(epoxide), and hence two electrons, formally transferred from the styrene, have to fill the iron heme orbitals. This can be done in two "installments" or in a single one. The interaction of Cpd I with styrene leads initially to a C—O bond between the FeO group and the terminal carbon atom of styrene. As a result, the benzylic carbon position becomes either a radical, with a singly occupied orbital labeled as φ_C, or a cationic center. In the first case, the heme gains one electron, which can fill either one of the a$_{2u}$, π^*_{xz} or π^*_{yz} orbitals to form a radical intermediate (**2**$_{rad}$). Alternatively, the cationic intermediate (**2**$_{cat}$) is formed via an additional electron transfer, from the radical center, to one of the orbitals in the, a$_{2u}$, π^*_{xz}, π^*_{yz}, $\sigma^*_{z^2}$, or σ^*_{xy} manifold.[34,36] Thus, many options for creating an intermediate complex are possible, with different electromeric situations (oxidation states on Fe and Por) and spin states. The ordering of these intermediates depends on environmental factors such as polarity and hydrogen bonding.[36,37,47,48] Figure 2 summarizes the low-lying states of the ^{4,2}**2**$_{cat}$ and ^{4,2}**2**$_{rad}$ species, where the Roman numerals, for example, **2**-IV, indicate the oxidation state of iron. The letter combinations (*xz*, *yz*, etc) indicate orbital occupancy in **2**$_{cat}$; in the doublet state cationic species, this indicates the identity of the singly occupied orbital on iron, whereas in the quartet spin state, this is the orbital that accommodates the electron transferred from the φ_C orbital on radical center in ^{4}**2**-IV.

Intermediates en route to styrene activation by Cpd I: Figure 3 shows relative energies of different radical and cationic intermediates under different environmental conditions. Initially, in the gas-phase there are four low-lying intermediates all within 1 kcalmol^{-1} of each other; two of these are radical in character (^{4,2}**2**$_{rad}$-IV) and two cationic (^{2}**2**$_{cat,xz}$;
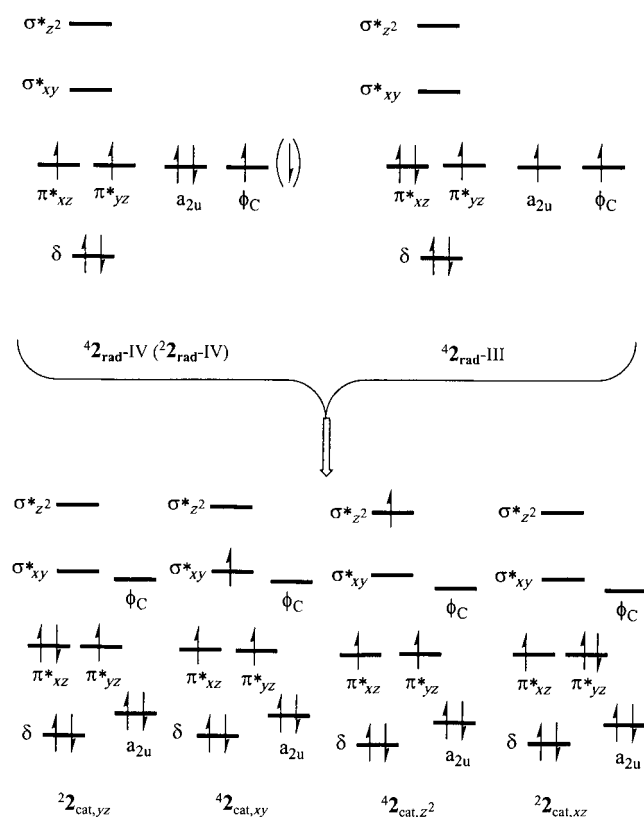
$\sigma^*_{z^2}$ —— $\sigma^*_{z^2}$ ——

σ^*_{xy} —— σ^*_{xy} ——

π^*_{xz} π^*_{yz} a_{2u} φ_C π^*_{xz} π^*_{yz} a_{2u} φ_C

δ δ

$^4\mathbf{2}_{rad}\text{-IV}$ $(^2\mathbf{2}_{rad}\text{-IV})$ $^4\mathbf{2}_{rad}\text{-III}$

$\sigma^*_{z^2}$ —— $\sigma^*_{z^2}$ —— $\sigma^*_{z^2}$ —— $\sigma^*_{z^2}$ ——

σ^*_{xy} —— σ^*_{xy} —— σ^*_{xy} —— σ^*_{xy} ——
φ_C φ_C φ_C φ_C

π^*_{xz} π^*_{yz} π^*_{xz} π^*_{yz} π^*_{xz} π^*_{yz} π^*_{xz} π^*_{yz}

δ a_{2u} δ a_{2u} δ a_{2u} δ a_{2u}

$^2\mathbf{2}_{cat,yz}$ $^4\mathbf{2}_{cat,xy}$ $^4\mathbf{2}_{cat,z^2}$ $^2\mathbf{2}_{cat,xz}$

Figure 2. Orbital occupancy of various $\mathbf{2}_{rad}$- and $\mathbf{2}_{cat}$-type states potentially encountered after C–O bond formation *en route* to C=C epoxidation. The heme orbitals are specified as in Figure 1, and φ_C is the orbital on the benzylic carbon of styrene.

$^2\mathbf{2}_{cat,yz}$). The two cationic species, $^2\mathbf{2}_{cat,xz}$ and $^2\mathbf{2}_{cat,yz}$, are stabilized relative to the radical states in a dielectric environment but are disfavored by the NH–S hydrogen bonding as such. Adding the dielectric effect to the NH–S hydrogen bonding establishes these species as the lowest energy intermediates. The high-spin cationic states ($^4\mathbf{2}_{cat,z^2}$ and $^4\mathbf{2}_{cat,xy}$) are well above the radical intermediates even under environmental conditions. Another radical-state but with the iron in oxidation state Fe^{III} ($^4\mathbf{2}_{rad}$-III) with occupation $(\pi^*_{xz})^2 (\pi^*_{yz})^1 (a_{2u})^1 (\varphi_{Alk})^1$ is 5.4 kcal mol^{-1} above the lowest lying state with inclusion of the environmental effects. Judging from experience with these states in camphor hydroxylation,[49] the $^4\mathbf{2}_{rad}$-III intermediate might be even closer to $^4\mathbf{2}_{rad}$-IV than the picture in Figure 3 might reveal. As shown later, these states play a key role by mediating the side products. Clearly then, we can expect multistate reactivity[50–52] in which the various products will arise from the interplay of two spin states and different electromeric situations.

Figure 4 shows group spin densities and degree of charge-transfer (Q_{CT}) for the four lowest-lying intermediates, that is, $^{4,2}\mathbf{2}_{rad}$-IV, $^2\mathbf{2}_{cat,xz}$ and $^2\mathbf{2}_{cat,yz}$. It can be seen that the cationic intermediates, in fact, are not purely cationic since significant spin density remains on the substrate: $\rho_{Alk}=0.68$ ($^2\mathbf{2}_{cat,yz}$) and $\rho_{Alk}=0.58$ ($^2\mathbf{2}_{cat,xz}$). This is because there is considerable mixing between the "empty" orbital on the substrate (φ_C) and the porphyrin type a_{2u} orbital leading to partially occupied orbitals and natural orbital occupancies deviating from integer values.[39] When the species are calculated in the presence of a dielectric medium and two NH–S hydrogen bonds, the radical character on the alkyl group decreases and the charge transfer exceeds 0.6; the two species are tight ion pairs with a significant delocalization of the charge.[39,53] Under all environmental conditions there is spin density of unity on the iron, which has an Fe^{III} oxidation state. In contrast, in the $^{4,2}\mathbf{2}_{rad}$ species, the spin density on the alkyl moiety is close to unity and the degree of charge transfer is substantially lower: ~0.3. In the latter two species, the spin density on iron is close to two, which corresponds to an Fe^{IV} oxidation state.

Rotational barriers in the intermediates: To address the stereospecificity of epoxidation (e.g., starting from *trans*-2-deuterio-styrene), we calculated the rotational barrier around the C–C bond of the intermediate, $^4\mathbf{2}_{rad}$-IV. The resultant rotational barrier that leads to scrambling was found to be 1.3 kcal mol^{-1} (see Figure S14 in the Supporting Information), which is presumably the same for all other species, as found previously.[34,35] Thus, any intermediate with a barrier for ring closure exceeding the rotational barrier will lead to epoxides with scrambled stereochemistry.

Mechanism of styrene epoxidation: We ran extensive geometry scans between intermediates and reactants for all intermediates depicted in Figure 3, in order to test their connection to the epoxide product (see Figure S6 in the Supporting Information). The geometry scans, however, starting from $^4\mathbf{2}_{cat,z^2}$, $^4\mathbf{2}_{cat,xy}$ and $^2\mathbf{2}_{cat,xz}$ all are connected to an excited state of Cpd I and styrene and consequently will not participate in epoxide formation. The three lowest-lying reaction pathways from ^{4,2}Cpd I are non-synchronous, and lead initially to two radical intermediates ($^{4,2}\mathbf{2}_{rad}$-IV) and a cationic intermediate ($^2\mathbf{2}_{cat,yz}$), which are depicted in Figure 5. In the gas-phase, the lowest lying pathway is via ^{4}TS1$_{rad}$ and is only 8.5 kcal mol^{-1} above the energy of separated reactants while the barriers ^{2}TS1$_{rad}$ and ^{2}TS1$_{yz}$ are only 0.7 and 1.1 kcal mol^{-1} higher. The computed free energy for this reaction via ^{4}TS1$_{rad}$ is $\Delta G^{\ddagger}=20.9$ kcal mol^{-1} which compares reasonably well with the experimental value of 24–25 kcal mol^{-1} reported by Vaz et al.[19] for the epoxidation of styrene by P450$_{cam}$.

The various intermediates in Figure 5 undergo subsequent ring closure to afford the epoxide complex. As before,[34,37] here too, the low-spin surfaces are effectively concerted pathways without a ring-closure barrier to form the product. By contrast, the high-spin pathway via $^4\mathbf{2}_{rad}$-IV encounters a small barrier (^{4}TS2-IV) for ring closure of 1.6 kcal mol^{-1}. A much larger barrier of 7.3 kcal mol^{-1} (^{4}TS2-III) is found for $^4\mathbf{2}_{rad}$-III, which is almost identical to the one obtained with ethylene[34] as a substrate, that is, 7.2 kcal mol^{-1}.

In accord with previous studies[34,37] here too, for the bare molecules ("gas-phase" conditions) the bond-activation phase has a somewhat lower barrier on the high-spin surface than on the low-spin surface. Calculating the relative ener-
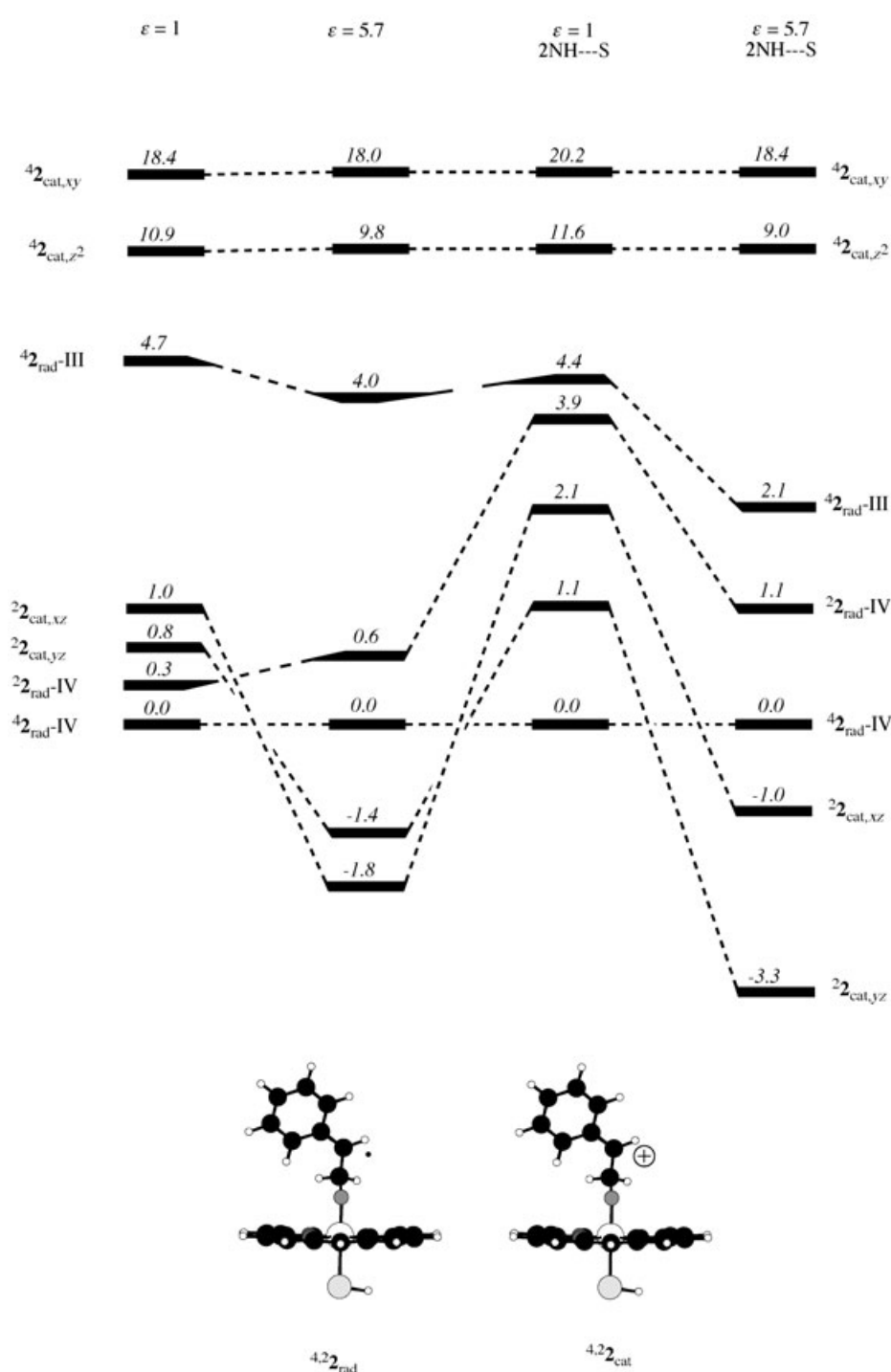
Figure 3. Relative energies of possible radical (2_{rad}) and cationic intermediates (2_{cat}) in the gas-phase ($\varepsilon = 1$), in a dielectric medium ($\varepsilon = 5.7$), in the gas-phase with two hydrogen bonded ammonia molecules and with the two external perturbations combined. All energies are in kcalmol^{-1} relative to $^4 2_{rad}$-IV intermediate.

gies of $^{4,2}TS1_{rad}$ and $^2TS1_{yz}$ under external perturbations changed this ordering, and the results are depicted in Figure 6. Although, in the gas-phase the preference is for the high-spin species, hydrogen bonding and a dielectric medium switch the preference to the low-spin ones. With both effects combined, the LS pathways are 3.5–

3.7 kcalmol^{-1} more favored than the high-spin pathway. This reversal of high-spin and low-spin TSs was also observed for propene epoxidation, where the $^2TS1_{rad}$ became the lowest energy species.[37,47] However, with styrene, the external perturbations prefer the low-spin cationic pathway $^2TS1_{yz}$ that is connected to $^2 2_{cat,yz}$. Since the ring-closure from $^2 2_{cat,yz}$ is essentially barrier free, the lifetime of $^2 2_{cat,yz}$ will be too short to lead to anything else but to the epoxide complex without loss of stereochemical information (e.g., if the substrate starts as cis- or trans-2-deuteriostyrene).

Suicidal complex formation: One of the side products in alkene epoxidations by Cpd I is the formation of the so-called suicidal complex (**4**). The mechanism for this side reaction was studied before using ethene as a substrate.[35,36] It was shown to involve a surface crossing between the surfaces that emanate from the radical states, $^4 2_{rad}$-IV,III and the corresponding surface of the $^4 2_{cat,xy}$ state (See Figure 2 for electronic configuration). The potential energy landscape for the suicidal complex formation from the $^4 2_{rad}$-IV, $^4 2_{rad}$-III and $^4 2_{cat,xy}$ states is depicted in Figure 7. Indeed, as found before, here too the $^4 2_{cat,xy}$ falls in a barrier free manner to the suicidal complex, ^{4}**4**. By contrast, $^4 2_{rad}$-IV has to pass a considerable barrier of 15.4 kcalmol^{-1} via $^4TS3$ en route to ^{4}**4** (in fact the $^4 2_{cat,xy}$ surface should cross the $^4 2_{rad}$-IV surface slightly below $^4TS3$; see Figure S8 in the Supporting Information).[54] Since the ring-closure barrier via $^4TS2$-IV (Figure 5) is only 1.6 kcalmol^{-1} above $^4 2_{rad}$-IV, this intermediate will not participate in a suicidal complex formation. By contrast, the $^4 2_{rad}$-III intermediate has a significant barrier to ring closure, about 7.3 kcalmol^{-1}, which is comparable to its crossover barrier[54] to the suicidal complex formation. As such, some

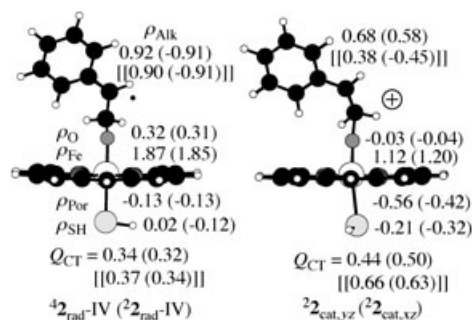Figure 4. Group spin densities (ρ) and degree of charge-transfer (Q_{CT}) of the four lowest lying intermediates in the activation of styrene. The data in the double brackets correspond to the species with 2NH—S hydrogen bonds and in a dielectric medium of $\varepsilon = 5.7$.

population of the $^4\mathbf{2}_{rad}$-III intermediate will lead to suicidal complex formation. This, however, will be a minor product considering the relative energy of the $^4\mathbf{2}_{rad}$-III to the $^2\mathbf{2}_{cat,yz}$ intermediates.

Phenacetaldehyde side products: Phenacetaldehyde side products are commonly observed in styrene epoxidation studies, sometimes even in yields of up to 16%.[8] A geometry scan (see Figure S13 in the Supporting Information) showed that a direct hydrogen transfer from the intermediates ($^4\mathbf{2}_{rad}$-IV; $^4\mathbf{2}_{rad}$-III) to form phenacetaldehyde is energetically demanding. Likewise attempts to scan the proton-transfer on the low-spin surface, starting from $^2\mathbf{2}_{cat,yz}$ en route to $^2\mathbf{5}$ led to rapid ring-closure to the epoxide complex.
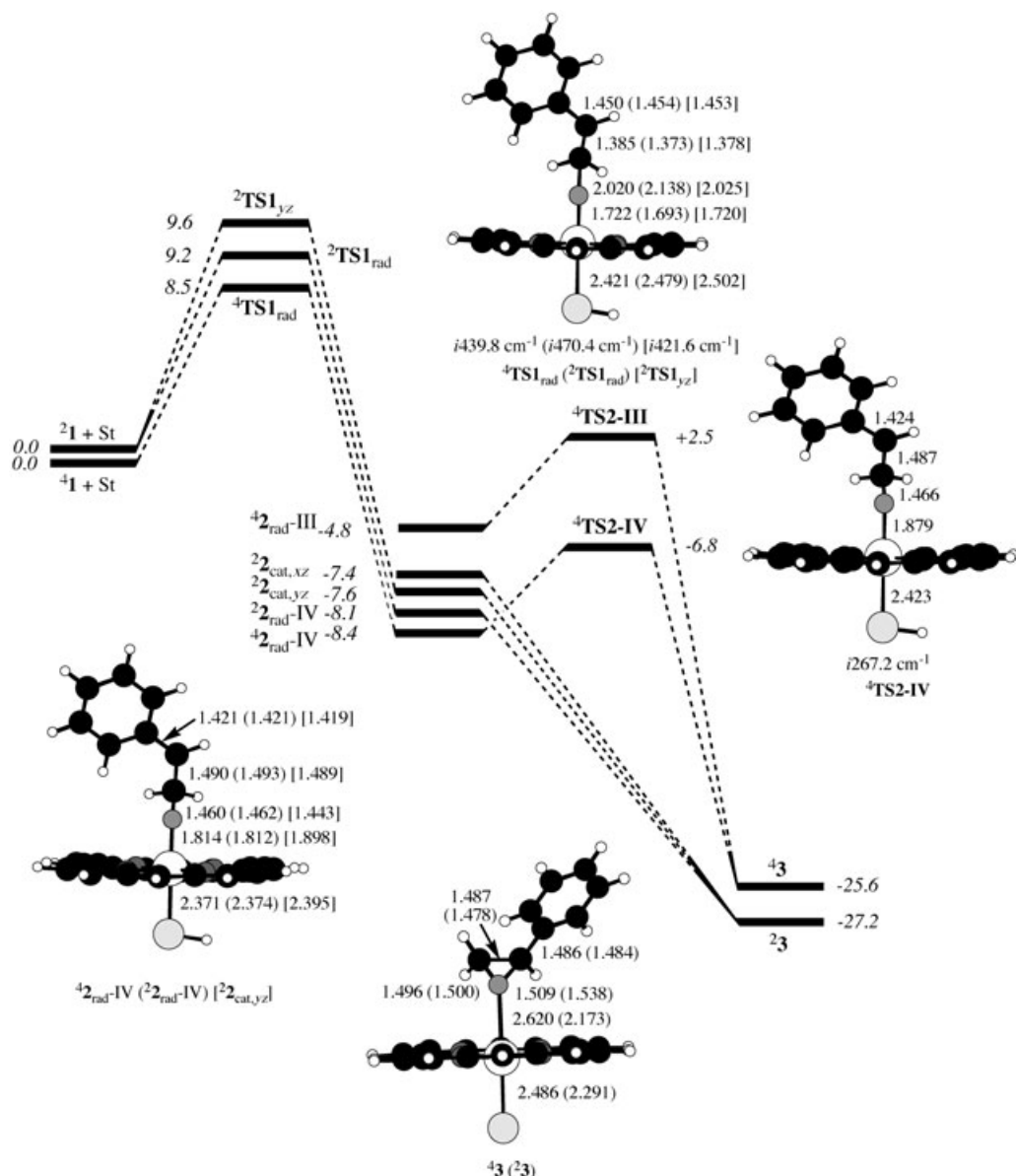

Figure 5. A multistate potential energy profile for the reaction of ^{4,2}Cpd I, $^{4,2}\mathbf{1}$, with styrene (St). The bond activation phase leads to the radical ($^{4,2}\mathbf{2}_{rad}$-IV, $^4\mathbf{2}_{rad}$-III) and cationic ($^2\mathbf{2}_{cat,yz}$) intermediates. In a subsequent phase, these species undergo ring closure to afford the epoxide complexes. All energies include zero-point corrections, are in kcal mol^{-1} relative to isolated reactants and are taken from the Gaussian frequency calculations. Key optimized geometric parameters are indicated near the structures.
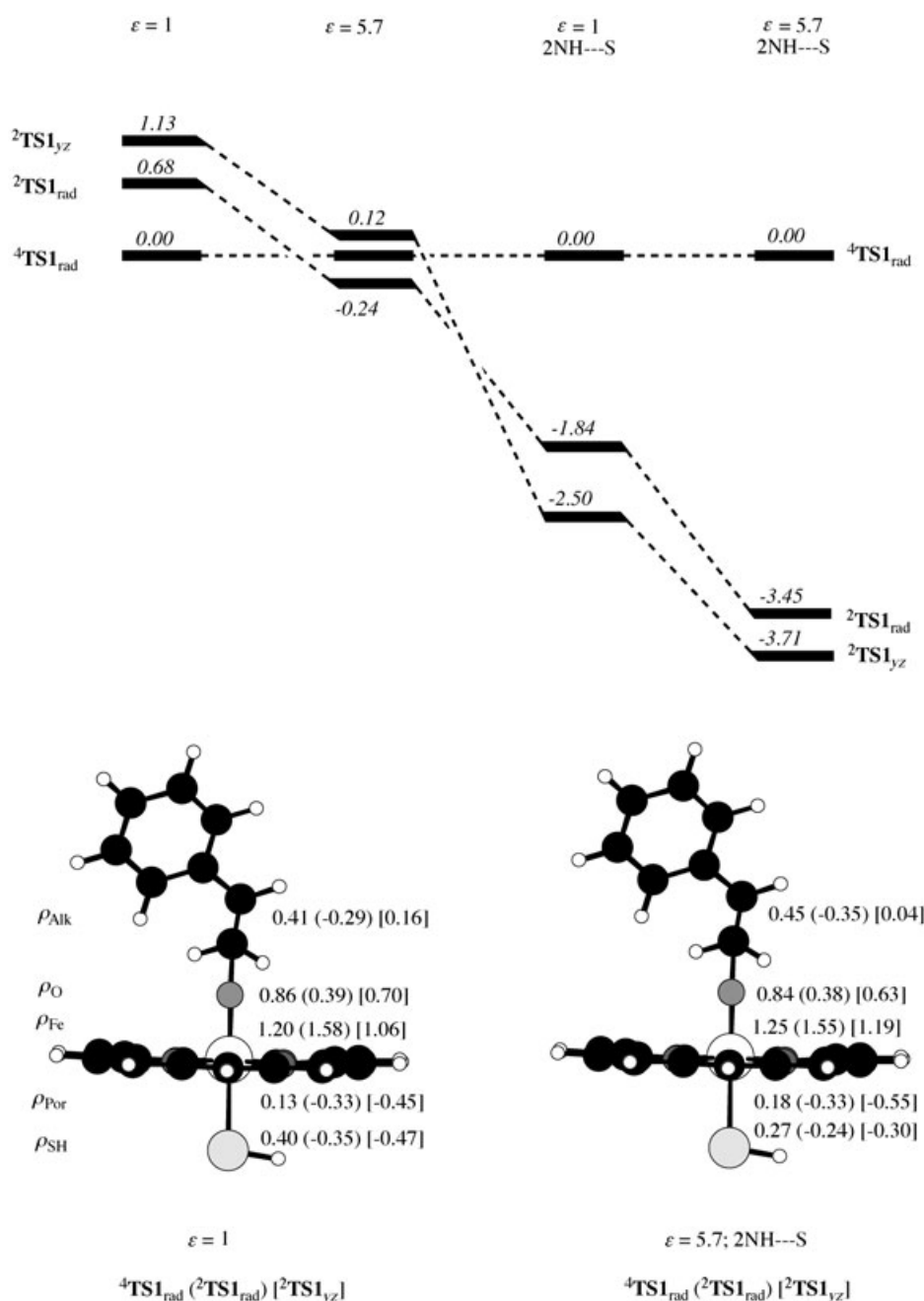
Figure 6. Relative energies of $^{4,2}TS1_{rad}$ and $^{2}TS1_{yz}$ in the gas-phase ($\varepsilon = 1$), in a dielectric constant of $\varepsilon = 5.7$, in the gas-phase with two hydrogen-bonded ammonia molecules and in a dielectric constant of $\varepsilon = 5.7$ with two hydrogen-bonded ammonia molecules. All energies are relative to $^{4}TS1_{rad}$ and include zero-point energy corrections. Also shown are the group spin densities in the gas-phase and in a dielectric constant of $\varepsilon = 5.7$ with two hydrogen-bonded ammonia molecules.

to the basic nitrogen atoms in the porphyrin ring. The potential energy profile for the formation of phenacetaldehyde from intermediates is depicted in Figure 8 alongside optimized geometries of the critical points. The mechanism is seen to involve a barrier free proton transfer, from the CH_2 group of the $PhCH_2CHO$ moiety to one of the nitrogens of the porphyrin ring to form the porphyrin protonated complex ($^{4}5$). Subsequently, the proton is reshuttled to the substrate into two sites. One leads to the aldehyde complex ($^{4}6$), the second to the enol complex, ferric-styrene-ol ($^{4}7$). Note that the proton reshuttle from $^{4}5$ to $^{4}7$ has a tiny barrier of only $0.6 \, \text{kcal mol}^{-1}$ ($^{4}TS5$) while the barrier to the aldehyde formation is $15.1 \, \text{kcal mol}^{-1}$ ($^{4}TS4$). The reason for these large differences is the initial distance between the NH proton in $^{4}5$ and the destination carbon benzylic CH group, which is $3.494 \, \text{Å}$; this distance is long even with reorientation of the $PhCHCH_2$ moiety, and demands a substantial barrier. The distance of the NH proton to the oxygen atom, on the other hand, is rather short, and the oxygen atom is more basic than the carbon atom. Therefore, if within the protein pocket $^{2}5$ achieves thermal equilibrium very quickly, the proton-shuttle will lead to styrene-ol that will subsequently rearrange to aldehyde assisted by water molecules in the pocket or on the protein surface. If however, $^{2}5$ cannot be thermalized quickly and contains some of the excess energy, which the system has originally

in the onset point, then the aldehyde will form directly and retain the original hydrogen species of the styrene.

The entire mechanism for the formation of **7** and **6** involves surface crossing of $^{4,2}2_{rad}$-IV or $^{4,2}2_{rad}$-III to $^{4,2}2_{cat,z^2}$, as shown in Figure 8.[54] However, starting from $^{4}2_{rad}$-IV the crossover barrier is too high compared with the respective ring-closure barrier. Thus, $^{4}2_{rad}$-IV will not participate in al-
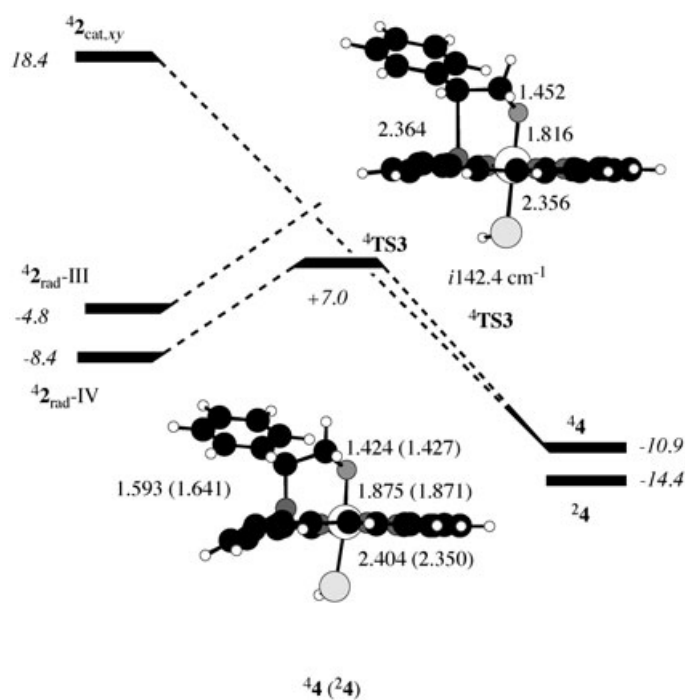
Therefore, as already stated, the low-spin cationic intermediate will be too short lived to rearrange to aldehyde side products.

The only pathway that was located started from $^{4}2_{cat,z^2}$ and continued to the side products in a barrier free manner. The mechanism is analogous to the one found for benzene hydroxylation[48] by P450, and is mediated via a proton-shuttle

Figure 7. Potential energy profile and optimized geometries of the formation of the suicidal complex (^{4}**4**) from ^{4}**2**$_{rad}$-IV, ^{4}**2**$_{rad}$-III and ^{4}**2**$_{cat,xy}$. All energies are relative to isolated reactants in kcal mol^{-1} and, wherever possible, include zero-point corrections. Bond lengths are in Å.

dehyde production. However, starting from ^{4}**2**$_{rad}$-III the corresponding crossover barrier and the ring closure barrier are of the same order and hence, the aldehyde byproduct will be formed from the ^{4}**2**$_{rad}$-III intermediate only.

Discussion

Since the TSs of the bond activation phase (Figure 5) are considerably higher in energy than the intermediates, all the low-lying intermediates including ^{4}**2**$_{rad}$-IV and ^{4}**2**$_{rad}$-III may be populated (e.g., by bifurcations and spin crossovers) and will participate in product formation. The products will be formed from each intermediate state by competing pathways, which are: C–C rotation, ring closure, hydrogen shift, heme-alkylation, and spin crossover between the two spin manifolds. This is a complex situation with a few unknowns, especially with respect to the factors that determine the rates of spin crossover. Setting aside this latter issue, what will determine the relative yields are the relative barriers for the chemical processes for each intermediate state. The picture that emerges involves multistate reactivity (MSR) with state and spin specific product formation, and where the low-spin pathways yield epoxides with conserved stereochemistry while the high-spin pathways generate stereochemically scrambled epoxides and various side products.

An overview of possible reaction paths: Figure 9 summarizes the MSR reaction pathways of Cpd I with a stereochemically labeled styrene, for example, *trans*-2-deuteriostyrene. An initial bond activation step leads to the formation of four lower lying intermediates, ^{4,2}**2**$_{rad}$-IV, ^{4}**2**$_{rad}$-III, and ^{2}**2**$_{cat,yz}$. Since the ring-closure processes are essentially barrier free for the low-spin intermediates, these intermediates will lead only to epoxide formation, with conservation of the initial configuration of the *trans*-2-deuteriostyrene.

By contrast, to the low-spin species, the high-spin intermediates have ring-closure barriers and may therefore possess sufficiently long lifetime to undergo either C–C rotation before ring closure, thereby leading to stereochemically scrambled epoxide complexes, or to skeletal rearrangements, which generate side products. The C–C rotational barrier in ^{4}**2**$_{rad}$-IV is of the same order as the ring-closure barrier for this state. Consequently, this state will lead to stereochemically scrambled *cis* and *trans* epoxides. The amount of scrambling will be proportional to the population of the ^{4}**2**$_{rad}$-IV intermediate and to the effect of protein pocket on the C–C rotation vis-à-vis the ring closure. The ^{4}**2**$_{rad}$-III intermediate, on the other hand, has a large barrier for ring closure, and as such it will participate in other processes, such as the formation of the suicidal complex and the aldehyde.

A surface crossing from the ^{4}**2**$_{rad}$-III radical surface to a cationic surface nascent from the ^{4}**2**$_{cat,z^2}$ state (with a $(\pi^*_{xz})^1$ $(\pi^*_{yz})^1$ $(\sigma^*_{z^2})^1$ configuration in the d block) leads to a proton-shuttle to the porphyrin ring and the subsequent generation of either 2-hydroxystyrene or phenacetaldehyde by-products. Since it involves states of different polarity, this crossover barrier may further decrease in the protein pocket. The generation of the aldehyde complex from the protonated porphyrin intermediate has a large barrier, and will be formed directly only if ^{4}**5** cannot achieve quickly thermal equilibrium and still possesses some of the excess energy of its reactant species (the species ^{4}**2** in Figure 8). In such a case, the original hydrogen atom of the CH$_2$ group will end in the aldehyde by-product, very similar to the NIH-shift observed in benzene.[3,7c] If, however, the excess energy is instantaneously absorbed by the protein, then the aldehyde will be formed from the enol with assistance of the water molecules in the pocket. To the best of our knowledge, an enol species has never been reported or may be was not sought for.

The suicidal complex, ^{4}**4**, is generated from the crossover of the ^{4}**2**$_{rad}$-III and ^{4}**2**$_{cat,xy}$ states. In the gas-phase, the crossover barrier is well higher than the epoxidation barrier. This may limit the production of the suicidal complex to a minimum.

Predictions for synthetic models: The results of our calculations show that Cpd I or P450 is intrinsically an efficient catalyst for oxygen transfer reactions toward styrene. The mechanistic scheme in Figure 9 is in general agreement with experimentally based mechanisms.[6,7a,8,10,13,33,55,56] Theory adds, however, a new dimension that is concerned with the spin- and state-selectivity of product formation. The scheme lends itself to some predictions in artificial systems. The amount and number of side products depends on the height
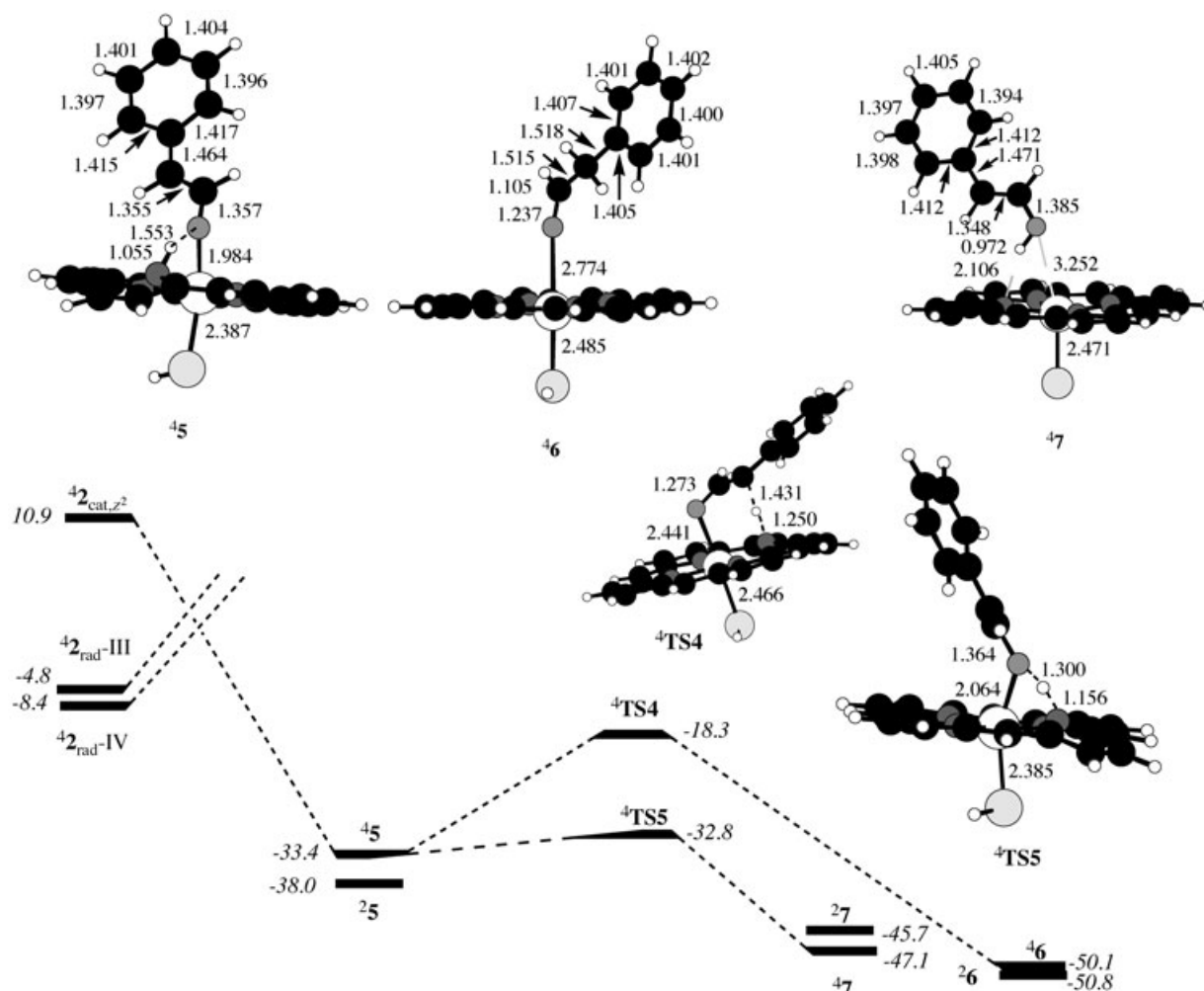
Figure 8. Relative energies (with respect to isolated reactants) and optimized geometries for the formation of phenacetaldehyde ($^{4,2}\mathbf{6}$) and 2-hydroxo-styrene ($^{4,2}\mathbf{7}$) via a proton-transfer intermediate ($^{4,2}\mathbf{5}$). Also shown are the structures of $^4\mathbf{TS4}$ and $^4\mathbf{TS5}$. All energies include zero-point correction and are relative to isolated reactants. Bond lengths of optimized geometries depicted are in Å.

of the crossover barriers, which in turn, depend on the heights of two orbitals that are populated in the $^4\mathbf{2}_{cat,xy}$ and $^4\mathbf{2}_{cat,z^2}$ states; the σ^*_{xy} orbital (leading to suicidal complexes) and the $\sigma^*_{z^2}$ orbital (leading to aldehydes). Thus, raising these orbitals in Cpd I will diminish the yield of side products, and vice versa. The $\sigma^*_{z^2}$ orbital depends critically on the nature of the axial ligand; this orbital is quite high for a thiolate ligand which is a strong binder of iron,[53] but will get much lower for a ligand such as imidazole, sulfates, and water, which are weaker iron binders.[53] The σ^*_{xy} orbital is not affected by changes in the axial ligand. However, both orbitals are strongly affected by replacing the iron by another transition metal. For example, ruthenium is a stronger binder than iron, and the corresponding σ^*_{xy} and $\sigma^*_{z^2}$ orbitals are very high, which should thereby minimize the side products.[57]

Since the amount of by-products depends on the population of the $^4\mathbf{2}_{rad}$-III intermediate, which possesses a singly occupied a_{2u} orbital, another possibility of reducing the amount of side products can be achieved by designing iron–porphyrin catalysts with low lying a_{2u} orbitals. In such cases,

the $^4\mathbf{2}_{rad}$-III intermediate with the singly occupied a_{2u} orbital will be much higher in energy than the $^4\mathbf{2}_{rad}$-IV intermediate, and will not be populated. Since the $^4\mathbf{2}_{rad}$-IV intermediate has a tiny barrier for ring closure more epoxide formation will follow. Replacement of the axial ligand (thiolate) with a weaker iron-binding ligand, such as water (chloride ion, etc) is one way. Another and more effective way is to substitute the porphyrin with electron withdrawing substituents, especially on the *meso* position. Such a substitution may altogether favor the low-spin cationic pathway (through $^2\mathbf{2}_{cat,yz}$), which is effectively concerted (See Figure 5). In cases where the $^4\mathbf{2}_{rad}$-IV intermediate is still populated such a substitution will lower the ring closure barrier and enhance the overall stereoselectivity of the epoxidation, thereby creating robust catalysts.

Summary and Conclusions

The reaction of styrene with Cpd I of P450 features multi-state reactivity (MSR) with different spin states (doublet
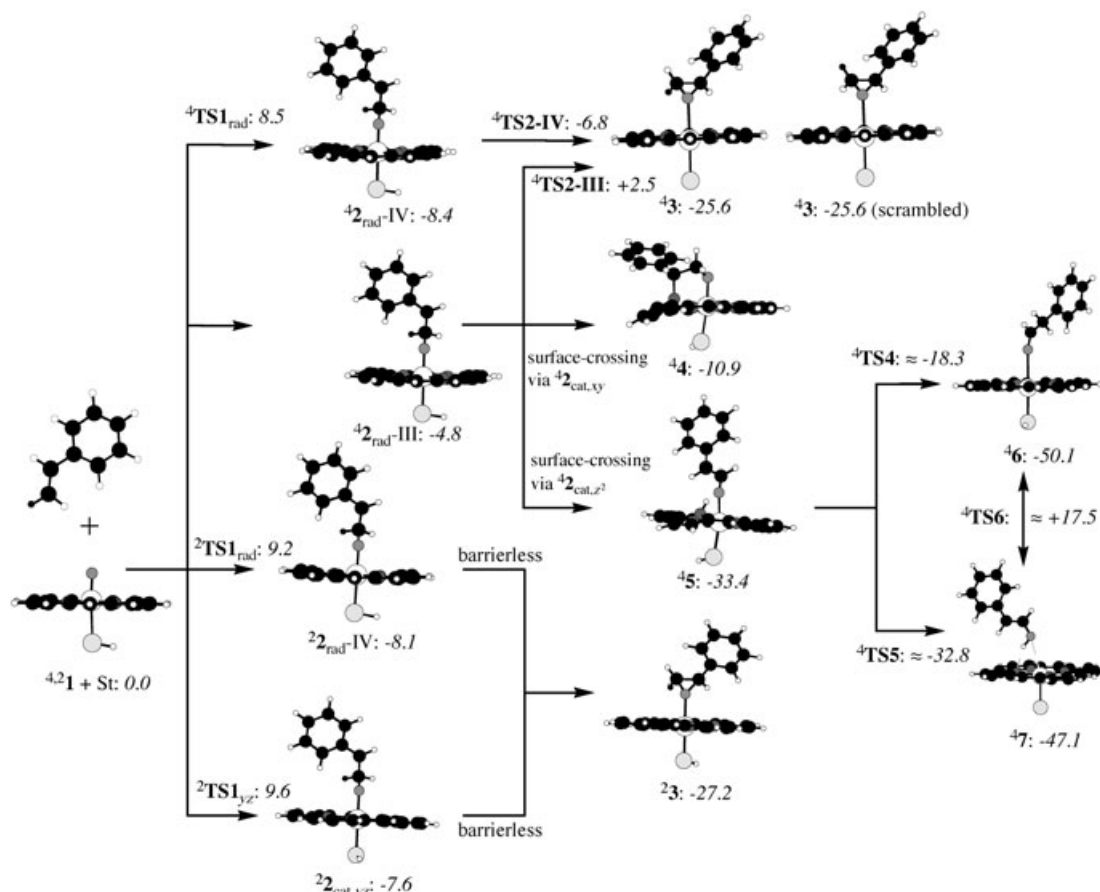
Figure 9. Multistate reactivity (MSR) in the reaction of *trans*-2-deuteriostyrene (St) with ^{4,2}Cpd I. The *trans* configuration of St is indicated by coloring the "deuterium" in black, whereas all the hydrogens are in white. The low-spin state leads to stereochemically conserved epoxide complex, ^{2}**3**. The high-spin states lead to stereochemically scrambled epoxide complex, ^{4}**3**$_{scramb}$, the suicidal complexes (^{4}**4**), phenacetaldehyde (^{4}**6**) and 2-hydroxostyrene (^{4}**7**). All energies are in kcal mol^{-1} relative to isolated reactants and include zero-point corrections. See reference [54] regarding the crossover barriers.

and quartet) and different electromeric situations having carbon radicals and cations, and different oxidation states on iron, Fe^{III} and Fe^{IV}. The mechanisms involve state-specific product formation, along the following inventory:

a) All the low-spin pathways lead to epoxide formation in effectively concerted mechanisms, albeit nonsynchronous ones.

b) The high-spin pathways have finite barriers for ring-closure and may have a sufficiently long lifetime to undergo rearrangement and lead to side products.

c) The high-spin radical intermediate, ^{4}**2**$_{rad}$-IV, has a ring closure barrier on the same order as the C–C rotation barrier, and will therefore lead to a mixture of *cis* and *trans* epoxides, starting from any one of the isomers (e.g., in 2-deuteriostyrene). The barriers for the production of aldehyde and suicidal complexes are too high for this intermediate.

d) The high-spin radical intermediate, ^{4}**2**$_{rad}$-III, has a substantial ring closure barrier and may survive long enough time to lead to suicidal, phenacetaldehyde and 2-hydroxostyrene side products.[54] All side products

have barriers, substantially higher than for the epoxide formation. Thus, in the gas-phase the amount of side products will be limited.

e) The phenacetaldehyde and 2-hydroxo-styrene products both originate from a cross-over from the ^{4}**2**$_{rad}$-III radical intermediate to the ^{4}**2**$_{cat,z^2}$ state. The process involves an *N*-protonated porphyrin intermediate that reshuttles the proton back to the substrate to form either phenacetaldehyde or 2-hydroxostyrene products. This resembles the internally mediated NIH-shift observed during benzene hydroxylation.

The theoretical scheme lends itself to some predictions, which were outlined above. However, the greater challenge is to find ways to probe this state and spin specific MSR scheme.

Acknowledgements

[1] *Cytochrome P450: Structure, Mechanism and Biochemistry*, (Ed.: P. R. Ortiz de Montellano), 2nd ed., Plenum Press, New York, **1995**.

[2] W.-D. Woggon, *Top. Curr. Chem.* **1997**, *184*, 39–96.

[3] M. Sono, M. P. Roach, E. D. Coulter, J. H. Dawson, *Chem. Rev.* **1996**, *96*, 2841–2887.

[4] *The Porphyrin Handbook* (Eds.: K. M. Kadish, K. M. Smith, R. Guilard), Academic Press, San Diego, CA, **2000**.

[5] F. P. Guengerich, *Chem. Res. Toxicol.* **2001**, *14*, 611–650.

[6] J. T. Groves, Y.-Z. Han in *Cytochrome P450: Structure, Mechanism and Biochemistry* (Ed.: P. R. Ortiz de Montellano), *2nd ed.*, Plenum Press, New York, **1995**, Chapter 1, pp. 3–48.

[7] a) F. P. Guengerich, T. L. MacDonald, *Acc. Chem. Res.* **1984**, *17*, 9–16; b) P. R. Ortiz de Montellano, J. J. De Voss, *Nat. Prod. Rep.* **2002**, *19*, 477–493; c) P. R. Ortiz de Montellano in *Cytochrome P450: Structure, Mechanism and Biochemistry* (Ed.: P. R. Ortiz de Montellano), 2nd ed., Plenum Press, New York, **1995**, Chapter 8, pp. 245–303.

[8] J. T. Groves, R. S. Myers, *J. Am. Chem. Soc.* **1983**, *105*, 5791–5796.

[9] J. T. Groves, Y. Watanabe, *J. Am. Chem. Soc.* **1986**, *108*, 507–508.

[10] J. P. Collman, T. Kodadek, J. I. Brauman, *J. Am. Chem. Soc.* **1986**, *108*, 2588–2594.

[11] J. P. Collman, J. I. Brauman, P. D. Hampton, H. Tanaka, D. S. Bohle, R. T. Hembre, *J. Am. Chem. Soc.* **1990**, *112*, 7980–7984.

[12] D. Mansuy, J. Leclaire, M. Fontecave, P. Dansette, *Tetrahedron* **1984**, *40*, 2847–2857.

[13] D. Ostovic, T. C. Bruice, *J. Am. Chem. Soc.* **1989**, *111*, 6511–6517.

[14] Z. Gross, S. Nimri, *J. Am. Chem. Soc.* **1995**, *117*, 8021–8022.

[15] Z. Gross, S. Ini, *Inorg. Chem.* **1999**, *38*, 1446–1449.

[16] Z. Gross, S. Ini, *Org. Lett.* **1999**, *1*, 2077–2080.

[17] A. M. D'A. Rocha Gonsalves, A. C. Serra, *J. Chem. Soc. Perkin Trans. 2* **2002**, 715–719.

[18] J. A. Fruetel, J. R. Collins, D. L. Camper, G. H. Loew, P. R. Ortiz de Montellano, *J. Am. Chem. Soc.* **1992**, *114*, 6987–6993.

[19] A. D. N. Vaz, D. F. McGinnity, M. J. Coon, *Proc. Natl. Acad. Sci. USA* **1998**, *95*, 3555–3560.

[20] J. P. Collman, J. I. Brauman, B. Meunier, T. Hayashi, T. Kodadek, S. A. Raybuck, *J. Am. Chem. Soc.* **1985**, *107*, 2000–2005.

[21] J. T. Groves, R. Quinn, *J. Am. Chem. Soc.* **1985**, *107*, 5790–5792.

[22] J. T. Groves, M. K. Stern, *J. Am. Chem. Soc.* **1987**, *109*, 3812–3814.

[23] J. T. Groves, K.-H. Ahn, R. Quinn, *J. Am. Chem. Soc.* **1988**, *110*, 4217–4220.

[24] P. R. Ortiz de Montellano, J. A. Fruetel, J. R. Collins, D. L. Camper, G. H. Loew, *J. Am. Chem. Soc.* **1991**, *113*, 3195–3196.

[25] P. R. Ortiz de Montellano, H. S. Beilan, K. L. Kunze, B. A. Mico, *J. Biol. Chem.* **1981**, *256*, 4395–4399.

[26] K. L. Kunze, B. L. K. Mangold, C. Wheeler, H. S. Beilan, P. R. Ortiz de Montellano, *J. Biol. Chem.* **1983**, *258*, 4202–4207.

[27] P. R. Ortiz de Montellano, B. L. K. Mangold, C. Wheeler, K. L. Kunze, N. O. Reich, *J. Biol. Chem.* **1983**, *258*, 4208–4213.

[28] P. R. Ortiz de Montellano, R. A. Stearns, K. C. Langry, *Mol. Pharmacol.* **1984**, *25*, 310–317.

[29] P. R. Ortiz de Montellano, *Acc. Chem. Res.* **1987**, *20*, 289–294.

[30] T. Mashiko, D. Dolphin, T. Nakano, T. G. Traylor, *J. Am. Chem. Soc.* **1985**, *107*, 3735–3736.

[31] A. F. Dexter, L. P. Hager, *J. Am. Chem. Soc.* **1995**, *117*, 817–818.

[32] P. G. Debrunner, A. F. Dexter, C. E. Schulz, Y.-M. Xia, L. P. Hager, *Proc. Natl. Acad. Sci. USA* **1996**, *93*, 12791–12798.

[33] a) D. C. Liebler, F. P. Guengerich, *Biochemistry* **1983**, *22*, 5482–5489; b) R. E. Miller, F. P. Guengerich, *Biochemistry* **1982**, *21*, 1090–1097.

[34] S. P. de Visser, F. Ogliaro, N. Harris, S. Shaik, *J. Am. Chem. Soc.* **2001**, *123*, 3037–3047.

[35] S. P. de Visser, F. Ogliaro, S. Shaik, *Angew. Chem.* **2001**, *113*, 2955–2958; *Angew. Chem. Int. Ed.* **2001**, *40*, 2871–2874.

[36] S. P. de Visser, D. Kumar, S. Shaik, *J. Inorg. Biochem.* **2004**, *98*, 1183–1193.

[37] S. P. de Visser, F. Ogliaro, P. K. Sharma, S. Shaik, *J. Am. Chem. Soc.* **2002**, *124*, 11809–11826.

[38] F. Ogliaro, N. Harris, S. Cohen, M. Filatov, S. P. de Visser, S. Shaik, *J. Am. Chem. Soc.* **2000**, *122*, 8977–8989.

[39] D. Kumar, S. P. de Visser, P. K. Sharma, S. Cohen, S. Shaik, *J. Am. Chem. Soc.* **2004**, *126*, 1907–1920.

[40] a) A. D. Becke, *J. Chem. Phys.* **1992**, *96*, 2155–2160; b) A. D. Becke, *J. Chem. Phys.* **1992**, *97*, 9173–9177; c) A. D. Becke, *J. Chem. Phys.* **1993**, *98*, 5648–5652; d) C. Lee, W. Yang, R. G. Parr, *Phys. Rev. B* **1988**, *37*, 785–789.

[41] a) J. P. Hay, W. R. Wadt, *J. Chem. Phys.* **1985**, *82*, 299–310; b) R. A. Friesner, R. B. Murphy, M. D. Beachy, M. N. Ringlanda, W. T. Pollard, B. D. Dunietz, Y. Cao, *J. Phys. Chem. A* **1999**, *103*, 1913–1928; c) W. J. Hehre, R. Ditchfield, J. A. Pople, *J. Chem. Phys.* **1972**, *56*, 2257–2261.

[42] a) A. Altun, W. Thiel, *J. Phys. Chem. B*, **2005**, *109*, 1268–1280; b) J. C. Schöneboom, H. Lin, N. Reuter, W. Thiel, S. Cohen, F. Ogliaro, S. Shaik, *J. Am. Chem. Soc.* **2002**, *124*, 8142–8151.

[43] Jaguar 4.5, Schrödinger, Inc., Portland, OR, **2000**.

[44] M. J. Frisch, G. W. Trucks, H. B. Schlegel, G. E. Scuseria, M. A. Robb, J. R. Cheeseman, V. G. Zakrzewski, J. A. Montgomery Jr., R. E. Stratmann, J. C. Burant, S. Dapprich, J. M. Millam, A. D. Daniels, K. N. Kudin, M. C. Strain, O. Farkas, J. Tomasi, V. Barone, M. Cossi, R. Cammi, B. Mennucci, C. Pomelli, C. Adamo, S. Clifford, J. Ochterski, G. A. Petersson, P. Y. Ayala, Q. Cui, K. Morokuma, D. K. Malick, A. D. Rabuck, K. Raghavachari, J. B. Foresman, J. Cioslowski, J. V. Ortiz, A. G. Baboul, B. B. Stefanov, G. Liu, A. Liashenko, P. Piskorz, I. Komaromi, R. Gomperts, R. L. Martin, D. J. Fox, T. Keith, M. A. Al-Laham, C. Y. Peng, A. Nanayakkara, C. Gonzalez, M. Challacombe, P. M. W. Gill, B. G. Johnson, W. Chen, M. W. Wong, J. L. Andres, M. Head-Gordon, E. S. Replogle, J. A. Pople, Gaussian, Inc.: Pittsburgh, PA, **1998**.

[45] F. Ogliaro, S. P. de Visser, S. Cohen, J. Kaneti, S. Shaik, *ChemBioChem* **2001**, *2*, 848–851.

[46] F. Ogliaro, S. Cohen, S. P. de Visser, S. Shaik, *J. Am. Chem. Soc.* **2000**, *122*, 12892–12893.

[47] S. P. de Visser, F. Ogliaro, P. K. Sharma, S. Shaik, *Angew. Chem.* **2002**, *114*, 2027–2031; *Angew. Chem. Int. Ed.* **2002**, *41*, 1947–1951.

[48] a) S. P. de Visser, S. Shaik, *J. Am. Chem. Soc.* **2003**, *125*, 7413–7424; b) C. M. Bathelt, L. Ridder, A. J. Mulholland, J. N. Harvey, *Org. Biomol. Chem.* **2004**, *2*, 2998–3005.

[49] J. C. Schöneboom, S. Cohen, H. Lin, S. Shaik, W. Thiel, *J. Am. Chem. Soc.* **2004**, *126*, 4017–4034.

[50] S. Shaik, S. P. de Visser, F. Ogliaro, H. Schwarz, D. Schröder, *Curr. Opin. Chem. Biol.* **2002**, *6*, 556–567.

[51] S. Shaik, S. P. de Visser, D. Kumar, *J. Biol. Inorg. Chem.* **2004**, *9*, 661–668.

[52] S. P. de Visser, D. Kumar, S. Cohen, R. Shacham, S. Shaik, *J. Am. Chem. Soc.* **2004**, *126*, 8362–8363.

[53] S. Shaik, S. Cohen, S. P. de Visser, P. K. Sharma, D. Kumar, S. Kozuch, F. Ogliaro, D. Danovich, *Eur. J. Inorg. Chem.* **2004**, 207–226.

[54] As discussed already (ref. [35]), this crossover is an artifact of the monodeterminant nature of DFT. In a multiconfigurational treatment such a crossing would have been slightly avoided. In any event, we cannot obtain an accurate value for the height of the minimal energy crossing point. In the case of Figure 7, the crossing point should be less than half of the gaps between the respective states (assuming the potential energy curves can be approximated by parabolas, the height of the crossing point will be 1/4 of the gap).

[55] J. T. Groves, Z. Gross, M. K. Stern, *Inorg. Chem.* **1994**, *33*, 5065–5072.

[56] Z. Gross, S. Nimri, C. M. Barzilay, L. Simkhovich, *J. Biol. Inorg. Chem.* **1997**, *2*, 492–506.

[57] a) F. Ogliaro, S. P. de Visser, J. T. Groves, S. Shaik, *Angew. Chem.* **2001**, *113*, 2958–2962; *Angew. Chem. Int. Ed.* **2001**, *40*, 2874–2878; b) P. K. Sharma, S. P. de Visser, F. Ogliaro, S. Shaik, *J. Am. Chem. Soc.* **2003**, *125*, 2291–2300.